The effects of fines on the hydraulic properties of well graded materials

K.A. Kwa & J. Ghorbani
The University of Sydney, School of Civil Engineering

D. Airey
The University of Sydney, School of Civil Engineering

ABSTRACT: The maritime transportation of iron ore and other metallic ores has been of increasing concern as in recent years, several bulk carriers, their cargo and around 200 lives have been lost but the mechanics behind the liquefaction of the cargo is still not well understood. These cargoes are transported at relatively low densities below a certain Transportable Moisture Limit (TML) as specified in the International Maritime Solid Bulk Cargoes (IMSBC) standards to ensure that the ore's degree of saturation is less than 70%. Studies are currently investigating the cyclic unsaturated soil behaviour and the moisture movements that occur during liquefaction of moist ores that can be caused by wave rocking motions during maritime transportation. Determining the hydraulic properties is necessary in developing a constitutive model that captures the hydro-mechanical response of these materials when subjected to unsaturated cyclic loading conditions. The hydraulic properties, including the permeabilities and soil water characteristic curves (SWCCs), of materials similar in grading to the ores, containing a range of particle sizes less than 9.5 mm and fines ($<75\ \mu$m) contents of 18%, 28% and 60% will be presented and the implications of the measured properties on the likelihood of cargo liquefaction will be discussed.

1 INTRODUCTION

In the past 30 years, at least 24 large ore carriers with cargoes of lateritic and nickel ores have capsized (Rose 2014). While the reason for many of these losses is unknown, liquefaction of the ore leading to shifting of the cargo in the hold is suspected to have played an important role as movement of the cargo can cause a ship to progressively tilt, become unstable and thus likely to capsize. The mechanics leading to liquefaction is poorly understood and a particularly challenging aspect is in understanding the unsaturated soil mechanics when the moist cargo is loaded into the ship and subsequently subjected to severe cyclic loading conditions that can develop in large swells during storms. Ideally, the ores would be shipped dry, however, the ores are wetted during the mining and handling processes and due to the presence of fines (particles less than 0.075 μm in size) contain and retain some moisture. The presence of both the fines and moisture in the cargo and that it is also loaded into the hold and transported at relatively loose states is why the International Solid Bulk Cargoes (IMSBC) code categorises iron ore fines as a problematic cargo, prone to liquefaction. To prevent liquefaction of the cargo during transportation, these cargoes are transported below a certain Transportable Moisture Limit (TML) based on a Proctor Fagerberg Test (PFT). This is similar to a standard compaction test except that lighter compaction hammers are used to achieve representative densities for the ore materials when loaded onto the ship. The drop heights and hammer weights used by the Technical Working Group (TWG) that are used to produce the compaction energies for a PFT can be found in TWG (2013).

The densities produced by using the C and D compaction energies, summarised in Table 1, have been found to best represent the densities achieved in ores from the loading process and the TML for these PFTs result in limiting degrees of saturation of 70% and 80% respectively.

Table 1. Modified Proctor Fagerberg C and D hammer tests developed for iron ore (TWG 2013).

Hammer	Hammer-Weight (g)	Drop Height (cm)	Compaction Energy (kJ/m^3)
C	350	20	85.5
D	150	15	27.6

However, it is questionable whether using a TML based on a PFT is sufficient for preventing the liquefaction of the material during transportation (Atkinson & Taylor 1994; Munro & Mohajerani 2016). More rigorous testing and modelling is required to investigate how the density and degree of saturation affect the liquefaction behaviour of these materials.

Furthermore, understanding how the grading of these ores affects their liquefaction behaviour is another important factor as these ores have variable gradings that contain wide ranges of particle sizes less than 9.5 mm and significant fines contents.

Studies have been undertaken to investigate the cyclic liquefaction behaviour in soil materials similar in grading to the ores under saturated conditions (Kwa & Airey 2017). Currently, the unsaturated soil behaviour and the moisture movements in these materials when subject to wave rocking motions that result from severe storms during transportation is being investigated and a constitutive model that captures the hydro-mechanical response of the materials under unsaturated cyclic loading conditions is being developed. Determining the hydraulic properties of these materials is required to calibrate the hydraulic part of the model, a necessary initial step before the hydro-mechanical response of the material can be analysed. Therefore, in this paper, the saturated permeabilities, and SWCCs of three different materials with gradings similar to the ores, containing basalt aggregates with particle sizes from 9.5 mm to 2 μm and feldspar fines at fine contents of 18%, 28%, and 60%, as shown in Figure 1, were determined.

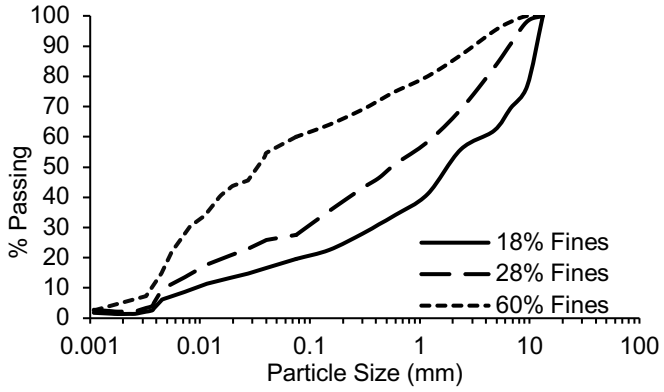

Figure 1. Grading curves.

A model has been developed to fit the SWCCs to the experimental data and the fitted SWCCs and permeability results were used to find the variation in the degree of saturation and resulting settlements in a one dimensional column.

2 EXPERIMENTS

2.1 *Permeability Testing*

Standard constant head permeability tests were performed on the materials, prepared as cylindrical samples 100 mm tall and 100 mm in diameter. Samples were prepared at void ratios associated with the TMLs where the 80% saturation line intersected the PFT D and C hammer compaction curves, determined as shown in Figure 2. The resulting void ratios for each material are summarised in Table 2. These samples were compacted in three layers in a split mould at the densities outlined in Table 1 and at moisture contents for which in disassembling the split mould and transferring the specimens to the apparatus, the samples did not collapse.

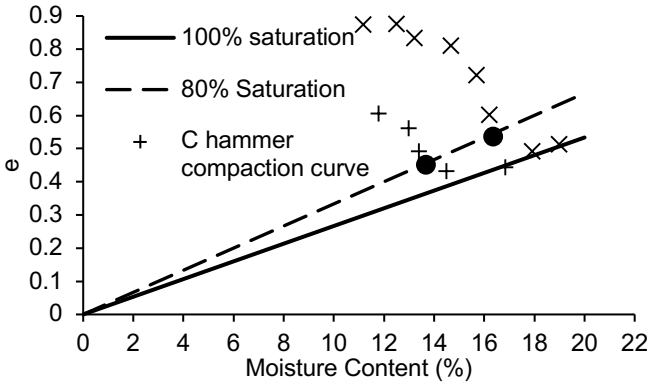

Figure 2. Typical selection method for the required densities for samples prepared using C and D compaction hammers (Kwa & Airey 2017).

Table 2. Void ratios used in preparation of samples.

% Fines	Compaction Hammer	e
18	C	0.26
	D	0.35
28	C	0.33
	D	0.4
60	C	0.45
	D	0.52

After mounting samples in the permeability apparatus, water was pumped in at the base to flush air out of the sample, using low pressures to ensure that the fines did not migrate through the samples. All samples were subsequently saturated at a low effective stress of 50 kPa to ensure that there was minimal change in the void ratio in the sample, and at elevated back pressures of 600 kPa. Samples were considered fully saturated when Skempton's B value was above 0.98. Various pressures differences ranging from 2 kPa to 15 kPa were applied at the top and bottom of the sample and the flow rates for different pressure differences were recorded. It was verified that the flow rate was proportional to the pressure difference consistent with Darcy's Law and hence the permeabilities determined, which are summarised in Table 3.

Table 3. Permeabilities (m/s).

Material	C hammer	D hammer
18% Fines	$3.83\text{x}10^{-6}$	$2.74\text{x}10^{-7}$
28% Fines	$3.80\text{x}10^{-8}$	$3.00\text{x}10^{-8}$
60% Fines	$4.50\text{x}10^{-8}$	$2.78\text{x}10^{-8}$

2.2 *Soil Water Characteristic Curves (SWCC)*

To find the materials' SWCCs, cylindrical samples 40 mm tall and 80 mm in diameter were tested in a con-

ventional pressure plate apparatus with a 3 bar ceramic high air entry porous disk capable of measuring suctions from 0 kPa to 200 kPa. Samples were prepared in three layers at the void ratios summarised in Table 2 and at moisture contents which resulted in the samples being close to fully saturated so that a drying curve could initially be established. Therefore, once samples were assembled in the apparatus, the air pressure applied at the top of the sample was increased while the water pressure supplied by a GDS pressure/volume controller and to the bottom of the sample through the ceramic disk, was kept constant. As suctions were increased, the volume of water coming out of the sample was recorded and displacements were measured by using an external linear variable differential transducer (LVDT). Once the samples reached equilibrium, which was when water ceased to flow through the sample at a specific suction and this generally occurred after 2-3 days, the suction was increased. After the maximum suction of 200 kPa was achieved, suction was incrementally reduced to find the wetting part of the samples' SWCC. During this stage of testing, the suctions were increased and subsequently decreased several times to established scanning curves between the drying and wetting curves, which are required for calibrating the model. The SWCCs for the three gradings are shown in Figures 3a, b and the data points used to define the scanning curves are shaded in black.

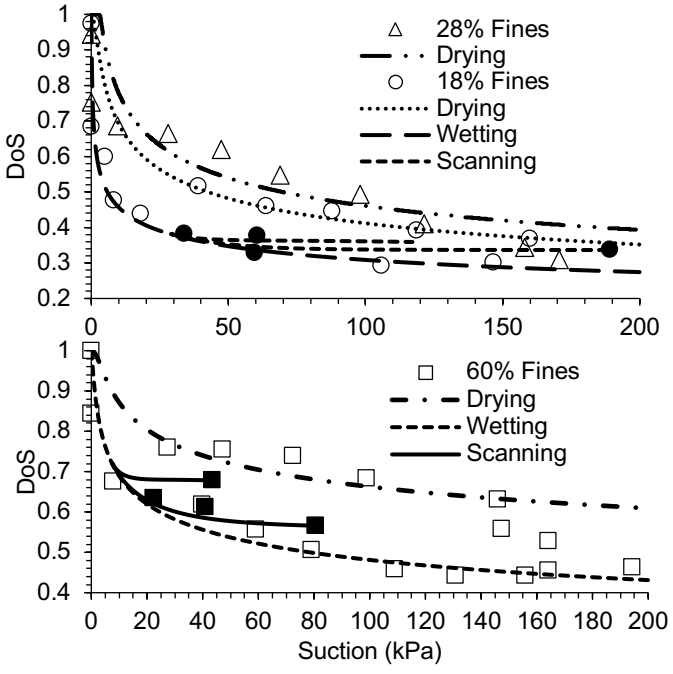

Figures 3. SWCCs: (a) 18% and 28% and (b) 60% fines.

3 MODEL

3.1 *SWCCs*

SWCCs have been observed to exhibit hysteresis when subjected to cycles of wetting and drying (Fredlund & Rahardjo 1993; Kato et al 1994; Tarantino & Tombolato 2005; Nuth & Laloui 2008) as well as in the materials used in this study. Therefore, a model that accurately simulates the unsaturated soil behaviour under cyclic loading needs to be able to successfully capture the hysteresis in the SWCCs. A complete SWCC can be idealised as having main wetting and drying curves and scanning curves which describe intermediate paths between them. To capture the possibility of modelling arbitrary paths for multiple drying/wetting processes, mentioned in Li (2005), and to avoid numerical problems which may arise upon drying/wetting reversals as discussed in Pedroso et al. (2015), a modified version of the approach proposed by Zhou et al (2012) is suggested where the slope of the SWCC in $S_e - p_c$ space, M^* is represented by Equation 1.

$$M^* = \left(\frac{p_c}{p_c^\alpha}\right)^{b_\alpha} \frac{\partial S_e^\alpha}{\partial p_c} + M^{*sc} \ (\alpha = w, d) \qquad (1)$$

where p_c is suction and S_e is the effective degree of saturation defined by Equation 2

$$S_e = \frac{S_w - S_{rw}}{S_{ra} - S_{rw}} \qquad (2)$$

where S_w is the degree of saturation, S_{rw} is the residual degree of saturation at extremely dry conditions, and S_{ra} is the residual degree of saturation when fully saturated. In this study, S_{rw} and S_{ra} are considered 0.0 and 1.0, respectively. b_w and b_d are model constants with negative and positive quantities in the wetting and the drying processes, respectively. In addition, by taking the equations of the main wetting and drying curves as S_e^w and S_e^d, p_c^α $(\alpha = w, d)$ is defined as follows in Equation 3.

$$p_c^\alpha = S_e^{\alpha - 1}, (\alpha = w, d) \qquad (3)$$

Moreover, M^{*sc} in Equation (1) is defined by Equation 4.

$$M^{*sc} = M^{*r} \left(\frac{p_c - p_c^\alpha}{p_c^r - p_c^\alpha}\right)^{b_{sc}} \qquad (4)$$

where b_{sc} is a model parameter and a positive quantity; and is introduced to control the shape of scanning curves at the initiation of a reverse

Table 5. SWCC parameters.

Parameters	n^d	m^d	P^d (Pa)	b^d	n^w	m^w	P^w(kPa)	b^w	b^{sc}
18% Fines	2.1	0.108	0.5	4.0	2.3	0.0074	0.1	-2.0	15
28% Fines	19	0.012	0.3	-	-	-	-	-	-
60% Fines	2.2	0.055	0.3	4.0	1.27	0.125	0.1	-2.0	20

process. p_c^r and M^{*r} are the values of suction and the slope of the SWCC once a reverse process is initiated. Equation 5, proposed by Van Genuchten (1980), was chosen for the main wetting and drying curves

$$S_e^\alpha = \left(1 + \left(\frac{p_c}{P^\alpha}\right)^{n^\alpha}\right)^{-m^\alpha} \quad (\alpha = w, d) \qquad (5)$$

where p^α is the air-entry value; and n^α and m^α are two model parameters. The resulting fitted SWCCs for each material are shown in Figures 3 a, b.

3.2 *Unsaturated Column*

Once the SWCCs were determined for each material, the SWCC parameters were used in a one dimensional unsaturated elastic analysis, performed on a column with dimensions 10 m height and 1 m in width. A schematic representation of the finite element mesh including the imposed boundary conditions is shown in Figure 4.

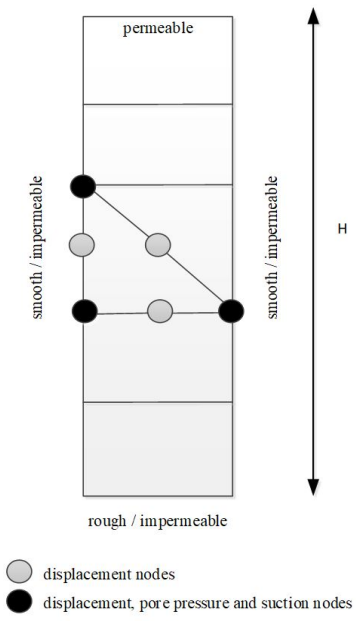

Figure 4. Schematic of one dimensional column.

Table 4. Material Parameters.

Parameter type	Symbol	Value	Unit
Porosity	n	0.3103	-
Density of the solid skeleton	ρ_s	2650	k gm^{-3}
Density of the water	ρ_w	997	kg m^{-3}
Density of the air	ρ_a	1.01	kg m^{-3}
Elastic modulus of the mixture	E	10.0	MPa
Poisson's ratio	ν	0.02	Pa
Bulk modulus of the water	K_w	2.25× 10^9	Pa
Bulk modulus of the air	K_a	1.10× 10^5	Pa
Intrinsic permeability	k	4.5 × 10^{-14}	m^2
Viscosity of the water	η_w	1.0× 10^{-3}	Ns m^{-2}
Viscosity of the air	η_a	1.8× 10^{-5}	Ns m^{-2}

The variation of the degree of saturation throughout the column with depth and the settlement results due to the application of body force were evaluated assuming the degree of saturation, suction relationship followed either the main drying, main wetting parts or scanning curves of the materials' SWCCs and the results are shown in Figures 5a, b, 6a, b and Table 6 respectively.

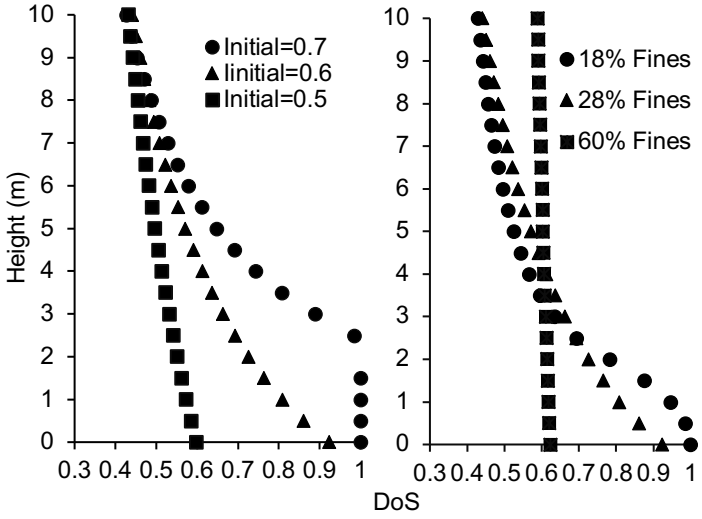

Figure 5. Variation in DoS with depth of the column with (a) increasing initial DoS for 28% fines and (b) increasing fines content at an initial DoS of 0.6.

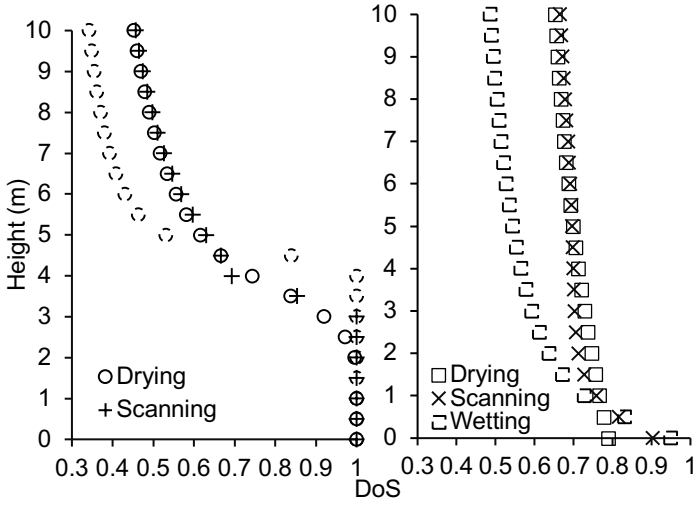

Figure 6. Variation in DoS with the depth of the column for: (a) 18% and (b) 60% fines given an initial DoS of 0.7 and initial states.

Table 6. Preliminary settlement results.

Material	SWCC	Settlement (mm)
18% Fines	Drying	27.38
	Wetting	27.1
	Scanning	27.36
28% Fines	Drying	37.78
60% Fines	Drying	44.89
	Wetting	50.14
	Scanning	56.25

4 ANALYSIS

The permeabilities measured in this study are consistent with the typical range of permeabilities that can be measured in gravelly sands which contain some fines. They were highest in the material containing the least amount of fines (18%) as this was the coarsest material and therefore, water flowed most easily through these samples. The permeabilities were very similar in the materials containing 28% and 60% fines and testing would have to be performed at different densities for clearer trends and differences to be observed between these materials.

As the fines content of the material was increased, the void ratios also increased as can be seen in the shifting up of the compaction curves in Figure 2. The changing fines content also affected the SWCCs of the materials, which shifted up and towards higher values of suction as the fines content was increased. In addition to the data shown in Figure 3 further tests were performed in the pressure plate apparatus with denser samples containing 18% and 60% fines and these showed the location of the SWCC, for a given fines content, was not dependent on the void ratio, which greatly simplified the model SWCC fitting process. Less hysteresis is observed in the SWCC of the material with 18% fines as the drying and wetting curves are much closer together compared to in the SWCCs for the material containing 60% fines. This is because a lower fines content results in water being able to flow more freely throughout the material during the drying and wetting processes, which is a result of the material containing 18% fines being more permeable, as summarised in Table 3. Due to time constraints, only the drying curve was determined for the material containing 28% fines, however, it is believed that the hysteresis in this material would be greater than in the material containing 18% fines, but less than in the material with 60% fines. The wetting and scanning parts of the SWCC for this material will be determined in the future. As can be seen in Figures 3 a, b, c, the drying, wetting and scanning parts of the SWCCs generated by the model generally fitted the experimental data well for each material. However, a limitation in the simulations of the SWCCs is that they did not capture the decrease in degree of saturation on the drying part of the SWCCs for materials containing 28% and 60% fines at suctions above 140 kPa however, as this was outside the range of suctions of interest in this study no attempt was made to further improve the SWCC fits. The drying and wetting air entry values for all of the materials were obtained during the SWCC fitting process and were found to be similar, approximately 2 kPa to 4 kPa and 0.1 kPa to 1 kPa respectively, which was consistent with the suctions measured in existing unsaturated triaxial data for this material as well as other studies that have been performed on similar materials (Gan & Fredlund 1997; Ng & Chiu 2003). These fitted SWCCs will be used in future simulations to analyse the hydro mechanical response of the unsaturated soil under cyclic loading conditions.

As expected in the analyses performed on the column of material, the degree of saturation increased with depth as water flowed from the top to the base of the column due to gravity. As can be seen in Figure 5a, for a particular material, the variation in the DoS was higher if a higher initial DoS was used in the analyses. It can be observed in Figure 5b that there was less variation in the DoS with depth in materials with higher fine contents as water redistributed less from the top to the bottom in these materials. This was because an increase in the fines content caused the material to have lower permeabilities and resulted in a shifting of the materials' SWCCs to higher degrees of saturation and values of suction. For an initial DoS of 0.7 the redistribution of water for the materials with lower fines contents resulted in the development of a wet base 4 m and 2 m thick for materials containing 18% and 28% fines respectively, as shown in Figures 6a and 5a. There was no development of a wet base in the material containing the highest, 60%, fines content for the selected initial DoS as water was not able to redistribute as freely, especially at lower degrees of saturation less than 0.6, because of the higher suctions present in this material. In the analyses the initial density and degree of saturation have been specified, however there is uncertainty in the initial suction state, as the materials could initially be on the wetting curve, the drying curve or on a scanning curve intermediate between these two lines. The results of the analyses shown in Figure 6 indicate that the assumed initial state can have a significant influence on the resulting DoS profiles. It is evident from Figures 6a and 6b, that there is more variation in the DoS with depth when the initial state lies on the wetting part of the SWCC. This occurs because lower suctions are associated with a particular DoS on the wetting part of the SWCC response and as a result water is also more likely to flow down from the top of the column due to gravity. Values of settlement can also be obtained from the simulations and are related to the elastic modulus of the material, obtained from existing triaxial data, and the pore water pressures which are related to the DoS that developed in the col-

umn during the analyses. However, because the settlements from these analyses are not significant they have not been included.

The movement of water towards the bottom of the column resulting in drying of the material at the surface and an increase in the DoS with depth, to possibly fully saturated conditions at the base as shown in the simulations, was consistent with centrifuge tests investigating liquefaction of materials in ships (Atkinson & Taylor 1994). They showed that the redistribution of water due to it flowing down as the cargo settled led to two principal mechanisms of instability in the cargo during transportation. Firstly, the rocking motions caused slope failures in the upper, drier portion of the cargo and secondly, when the saturated part at the base of the cargo was subject to cyclic loading, high pore pressures were generated which led to a loss of strength and resistance to the cargo shifting. However, the mechanical aspects of this model are still being developed and further investigation is required before the unsaturated behaviours relevant to liquefaction of the ores that can occur during their marine transportation can be analysed.

5 CONCLUSION

The SWCCs and permeabilities for materials similar in grading to metallic ores which are known to be prone to liquefaction during their shipping transportation, were determined and successfully used to calibrate the hydraulic part of the model being used in this study. The SWCCs were used in a one dimensional elastic analysis on a column of material and it was found that the fines content had a significant effect on the resulting varying degrees of saturation with depth. However, the model is still being developed and further work is required to simulate and investigate the effect of fines on the hydro-mechanical response of unsaturated materials similar in grading to metallic ores when subjected to cyclic loading conditions.

6 ACKNOWLEDGEMENTS

The authors acknowledge the support provided by the Australian Research Council Discovery Scheme (grant DP150103083).

7 REFERENCES

Atkinson, J.H., & Taylor, R.N. 1994. Moisture migration and stability of iron ore concentrate cargoes. *Centrifuge 94,* 1994 Balkema, Rotterdam.

Fredlund, D. G., & Rahardjo, H. 1993. Soil mechanics for unsaturated soils, John Wiley & Sons.

Gallipoli, D., Wheeler, S., & Karstunen, M. 2003. Modelling the variation of degree of saturation in a deformable unsaturated soil. *Géotechnique.* 53(1): 105-112.

Gan, J. K. M., & Fredlund, D. G. 1997. Study of the application of soil water characteristic curves and permeability functions to slope stability. *Final Rep.*, Civil Engineering Dept., Geotechnical Engineering Office, Hong Kong.

Ghorbani, J., Nazem, M., & Carter, J. 2016. Numerical modelling of multiphase flow in unsaturated deforming porous media. *Computers and Geotechnics* 71: 195-206.

Kato, S., Matsuoka, H., & Sun, D. 1995. A constitutive model for unsaturated soil based on extended SMP. *Proceedings of the first international conference on unsaturated soils 1995.* Volume 2.

Kwa, K.A., & Airey, D.W. 2017. The effects of fines on the liquefaction behaviour in well graded materials. *Can. Geotech. J.* 54(10): 1460-1471.

Li, X. (2005). Modelling of hysteresis response for arbitrary wetting/drying paths. *Computers and Geotechnics* 32(2): 133-137.

Munro, M., & Mohajerani, A. 2016. Moisture content limits of iron ore fines to prevent liquefaction during transport: review and experimental study. *International Journal of Mineral Processing* 148: 137-146.

Ng, C.W.W., & Chiu, A.C.F. 2003. Laboratory Study of loose saturated and unsaturated decomposed granitic soil. *Journal of Geotch. And Geoenviron. Eng.* 129(6): 550-559.

Nuth, M., & Laloui, L. 2008. Advances in modelling hysteretic water retention curve in deformable soils. *Computers and Geotechnics* 35(6): 835-844.

Pedroso, D. M., Sheng, D., & Zhao, J. 2009. The concept of reference curves for constitutive modelling in soil mechanics. *Computers and Geotechnics* 36(1–2): 149-165.

Rose, T.P. 2014. Thesis: Solid bulk shipping: cargo shift, liquefaction and the transportable moisture limit. *University of Oxford.*

Technical Working Group (TWG). 2013. TWG 3rd report and Imperial College review- Proctor Fagerberg (PF) Test, TWG 4th report and Imperial College review- Reference tests

Tarantino, A., & Tombolato, S. 2005. Coupling of hydraulic and mechanical behaviour in unsaturated compacted clay. *Géotechnique* 55(4): 307-317.

Zhou, A.N., Sheng, D., Sloan, S.W., & Gens, A. 2012. Interpretation of unsaturated soil behaviour in the stress–Saturation space, I: Volume change and water retention behaviour. *Computers and Geotechnics* 43: 178-187.

Van Genuchten, M.T. 1980. A closed-form equation for predicting the hydraulic conductivity of unsaturated soils. *Soil science society of America journal* 44(5): 892-898.